An Analytical Approach to Predict Maximal Sensitivity of Microring Resonators for Absorption Spectroscopy

Miguel Diez Garcia, Pauline Girault, Simon Joly, Laurent Oyhenart, Vincent Raimbault, Corinne Dejous, and Laurent Bechou

***Abstract*—The different biosensing strategies with microring resonators consist in quantifying the resonance shift under the presence of biological or chemical agents. These strategies lead to the measurement of a wavelength shift or an output power variation correlated to the analyte concentration. The design guidelines to enhance the sensitivity have been already studied and reviewed over the past decade. However, very few studies have been published addressing ring resonator performance used as absorption micro-spectrometer, which can be explored with colorimetric chemistry and microfluidic handling. In this work, a sensitivity model for the operation of absorptive based ring resonators is presented. Such a model is proposed to provide a guideline to optimize ring resonator design and parameters. Finally, 2.5 FDTD simulations of different ring geometries are presented and compared to the results obtained with the model.**

***Index Terms*—Absorption spectroscopy, biosensor, integrated optics, ring resonator.**

I. Introduction

VISIBLE absorption spectroscopy has been used for decades to determine the concentration of large amounts of components and reactions absorbing between 400–800 nm. Colorimetric reagents can be used in conjunction with optical devices such as optical fibers, to probe multiple analytes by measuring intrinsic absorption, or by incorporating sensing elements to enhance both selectivity and sensitivity [1].

Commercially available sensors based on optical fiber which rely on colorimetric absorption include CO_2 sensors in which a silica glass core is coated with a polymer cladding containing a colorimetric indicator. Upon exposure of any segment of the fiber, the CO_2 diffuses into the cladding and triggers a change in color [2], [3]. The same strategy can be used for sensing in aqueous media with the help of colorimetric reagents. For instance, direct absorption systems coupling LEDs and photodiodes with microfluidic channels are reported in [4], but the short optical absorption path strongly limits the sensitivity [5]. Nowadays, it has been established that optical ring resonators coupled with microfluidic chips can become feasible integration solutions for in-situ absorption spectroscopy [6], [7]. This type of optic-microfluidic assembly has been used at telecommunication wavelengths (1.55 μm) performing the sensing of different types of glucose and oils reported in [8], [9]. Microring resonators can be manufactured in the main visible platforms such as Si_3N_4 and curable polymers leading to highly integrated low-cost devices [10], [11].

Few studies have been also published exploring the use of microring resonators as micro-spectrometers. The cavity enhancement of light in a microring resonator enables to detect changes in its local environment. As recent application example, colorimetric sensing capabilities dedicated to Hexavalent Chromiun Cr(VI) detection was published by Meziane *et al.* [12]. Chromate ions reacts with diphenylcarbazide (DPC) showing variations of 10^{-6} on the imaginary part of the refractive index (extinction coefficient) for concentrations ranging from 5 μg/L to 1 mg/L. Based on the determination of the extinction coefficient, experimental measurements based on hollow-core metal-cladding optical waveguide sensor, puplished by Wang *et al.* [13], have shown variations in the extinction coefficient of the same magnitude order (10^{-6}). Nitkowsky *et al.* [14] also demonstrated experimentally the absorption performance of a Si_3N_4 microring resonator as biosensor by color-producing enzymatic reactions. Nevertheless, in all these studies, the consideration of sensitivity performance and the optimal geometry of the ring was never addressed for their use as colorimetric micro-spectrometers.

Microring resonators operating as micro-spectrometers for absorption sensing offer different and capabilities complementing the already well-understood strategies based on the refractive index shift. In this paper, we propose an analytical approach and a guideline to optimize ring resonator design and parameters studying its performance as microspectrometer, referring to an extension of experimental works already reported in literature. The sensitivity, defined as the ratio of power drop at resonance over the extinction coefficient variation, is discussed depending on the geometrical parameters of the ring. Then we report the optimization of the defined sensitivity regarding the light

Manuscript received May 16, 2019; revised July 23, 2019; accepted August 16, 2019. Date of publication August 28, 2019; date of current version November 1, 2019. *(Corresponding author: Pauline Girault.)*

M. D. Garcia, P. Girault, S. Joly, L. Oyhenart, C. Dejous, and L. Bechou are with the IMS Laboratory, University of Bordeaux, UMR CNRS 5218, Bordeaux INP, 351 Cours de la Libération, 33405 Talence, France (e-mail: miguel.diez-garcia@u-bordeaux.fr; girault pauline.pro@gmail.com; simon.joly@ims-bordeaux.fr; laurent.oyhenart@u-bordeaux.fr; corinne.dejous@ims-bordeaux.fr; laurent.bechou@u-bordeaux.fr).

V. Raimbault is with LAAS-CNRS, 31031 Toulouse, France (e-mail: vraimbau@laas.fr).

Color versions of one or more of the figures in this paper are available online at http://ieeexplore.ieee.org.

Digital Object Identifier 10.1109/JLT.2019.2938040

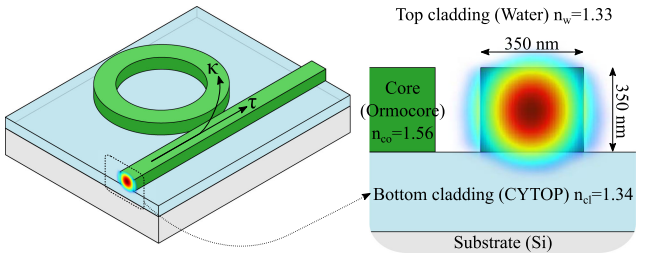

Fig. 1. Left: Proposed polymer single side coupled ring resonator. Self-coupling (τ) and cross-coupling (κ) coefficients are indicated. Right: Mode profile of the 350 nm $\times$ 350 nm polymer waveguide ($n_{co} = 1.56$) with a confinement factor $\Gamma_{core} = 0.65$.

coupling between the bus and ring waveguide. The optimal coupling configuration is analyzed taking into account the transmission of the unperturbed ring resonator and the ring resonator in presence of a lossy cladding. The role of the evanescent field, optical length and coupling mechanism is discussed. Finally, FDTD simulations (2.5D) of ring resonators are presented with different geometries to compare simulations results with the values obtained analytically.

II. Proposed Structure and Detection Principle

Commonly, two main sensing strategies can be found in literature, homogeneous sensing and surface sensing [15]. Mostly, they rely on the evanescent wave to detect analytes contained in the whole solution as in homogeneous sensing or oppositely, grafted on functionalized surfaces with dedicated binding as for surface sensing. In both cases, the main sensing strategy relies on a shift of the resonant wavelength due to the effective index modification of the propagated mode in the ring resonator. Alternatively, the shift of the resonance can be directly correlated to an output power variation collected by an appropriated photodiode and used to determine the analyte concentration.

By this way, absorption sensing using microring resonators and photodiodes has been demonstrated [16]. In the case of homogeneous sensing, the specificity of the sensor can be obtained externally with colorimetric chemistry and wavelength-tunable short-linewidth lasers. The measured power variation can be related to the absorption coefficient and thus, the concentration of the analyte.

The commonly used polymer-based structure is shown in Fig. 1. In this work, we have chosen a core with a refractive index n_{co} of 1.56 based on Ormocore polymer. The dimension of the waveguides are 350 nm $\times$ 350 nm ensuring single mode operation at visible wavelength ($\lambda = 532$ nm). The refractive index n_{cl} of the bottom cladding is chosen to match the refractive index of water ($n_w = 1.33$) which acts as top cladding. Perfluorinated polymers such a CYTOP provide good thermal stability with water-like refractive index ($n_{cl} = 1.34$) which is adequate for symmetric waveguide operation. The mode profile is depicted in Fig. 1(b) showing an effective index of 1.41 and power confinement factor Γ_{core} of 0.65. The complex refractive index of the top cladding is defined as $n_w + jn_i$. Here, the real part n_w is the refractive index and indicates phase velocity, while the imaginary part n_i is called the extinction coefficient. The

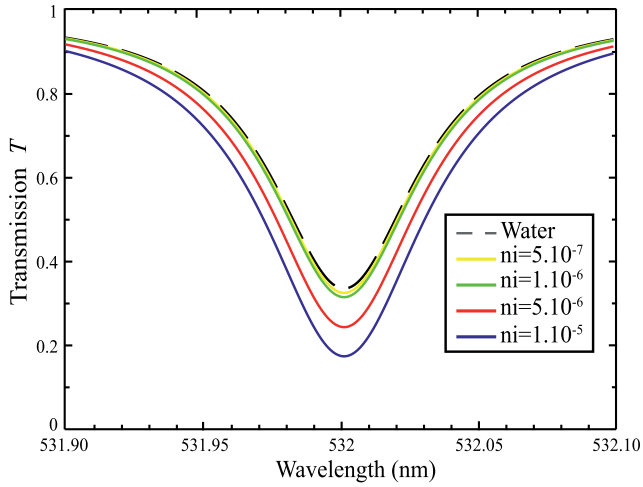

Fig. 2. Transmission spectrum of an all-pass ring resonator with a radius of 15 μm for different extinction coefficient variations.

colorimetric reaction only modifies the extinction coefficient n_i of the water top cladding considering $n_i \ll n_w$. Lumerical MODE solutions software was used to study the effect of the extinction coefficient variation on the top cladding of the resonators presented in this study. The MODE package provides a 2.5 dimensional tool to easily simulate the optical resonance of planar structures. This method is based in the collapse of the main slab mode in a 3D structure. The key assumption is based on negligible coupling between the different slab modes supported by the vertical waveguide structure. A typical response of ring resonator acting as a notch filter with 15 μm of radius is shown in Fig. 2. As water presents very low absorption in the visible region of the spectrum, no losses were considered for the reference water cladding in our model. Progressively, the top water cladding was modified increasing the extinction coefficient n_i ranging from 5.10^{-7} to 10^{-5} and decreasing the transmitted power at the resonance peak. Similarly, we can notice the decreasing of the quality factor ($Q = \frac{\lambda}{\delta\lambda}$) with the increase of the extinction coefficient. The modification of the extinction coefficient can be adapted depending on the reagent concentration used and the colorimetric indicator. Basically, the experimental extraction of the ring parameters can be achieved with a dedicated curve fitting of the transmission function or by directly measuring the power drop or the ON-OFF ratio, which is the power contrast between the power transmitted at resonance and out of resonance.

III. Analytical Model for Absorption Spectroscopy Sensing

A. Sensitivity

The theory underlying the operation of the ring resonator has been intensively described in the literature [17]. Here we consider the transmission function of a single side coupled ring resonator acting as a notch filter. From microring resonator equations, the transmission at resonance can be written as a function of the resonator coupling parameters as

follows:

$$T(n_i) = \frac{P_{out}(n_i)}{P_{in}} = \left(\frac{\tau - a(n_i)}{1 - \tau a(n_i)}\right)^2 \quad (1)$$

where P_{out} and P_{in} are the input and output power, τ is the self-coupling coefficient which represents the ratio of power remaining in the input waveguide and a represents the round-trip loss coefficient along the ring path L:

$$a^2 = e^{-\alpha(\Gamma, n_i)L} \quad (2)$$

α is the optical loss per unit length defined by $\alpha = \alpha_{bent} + \alpha_{prop}$. α_{bent} corresponds to the losses due to the bent radius while α_{prop} represents the losses due to the propagation inside the waveguide define as $\alpha_{prop} = \Gamma_{core}\alpha_{core} + \Gamma_{cladd}\alpha_{cladd}(ni) + \Gamma_{sub}\alpha_{sub} + \alpha_{rough}$. Each term corresponds to the intrinsic absorption of the core α_{core}, top cladding α_{cladd}, bottom cladding α_{sub}, and the scattering losses produced by the waveguide roughness α_{rough}.

The factors Γ_{core}, Γ_{cladd} and Γ_{sub} refer to the ratio of guided power in the core, in the top and bottom cladding respectively. All losses are fabrication-dependent except the top cladding losses which are affected by the absorption coefficient variations of the colorimetric complex.

Therefore, when Γ_{cladd} is large, the evanescent field extends into the lossy cladding increasing the total propagation loss. For a constant factor τ, the transmitted power is tuned by the propagation loss of the ring waveguide. In this case the round-trip loss coefficient a depends on the variable losses of the top cladding.

The sensitivity can be written in terms of power at resonance as:

$$S = \frac{P_{out}(n_i) - P_{out}(0)}{n_i P_{in}} \quad (3)$$

where P and n_i represent the optical power and the complex part of the refractive index (extinction coefficient) respectively. This equation represents the ratio of transmitted power loss due to a lossy perturbation added to the waveguide. For small variations of n_i, the equation can be approximated as follows:

$$S = \lim_{\Delta n_i \to 0} \frac{T(n_i + \Delta n_i) - T(n_i)}{\Delta n_i} \quad (4)$$

We can rewrite Eq. 4 as follows:

$$S = \frac{dT(n_i)}{dn_i} \quad (5)$$

The derivative of T with respect to the extinction coefficient n_i gives:

$$\frac{dT(n_i)}{dn_i} = \frac{d\alpha_{cladd}(n_i)}{dn_i} L\Gamma_{cladd} a \frac{(a-\tau)(1-\tau^2)}{(1-\tau a)^3} \quad (6)$$

The sensitivity depends on the round-trip loss coefficient a, the self-coupling coefficient τ and is proportional to the optical path and Γ_{cladd}. The absorption losses of the cladding coefficient α_{cladd} is related to the imaginary part of the refractive index n_i as follows:

$$\alpha_{cladd}(n_i) = \frac{4\pi n_i}{\lambda} \quad (7)$$

where we have only considered the influence of the absorption due to the lossy cladding. Therefore at $\lambda = \lambda_{res}$, equation 8 gives the final expression of the sensitivity:

$$S = \frac{dT(n_i)}{dn_i} = \underbrace{\frac{4\pi}{\lambda_{res}} L\Gamma_{cladd}}_{\text{Waveguide factor}} \underbrace{a\frac{(a-\tau)(1-\tau^2)}{(1-\tau a)^3}}_{\text{Enhancement factor}} \quad (8)$$

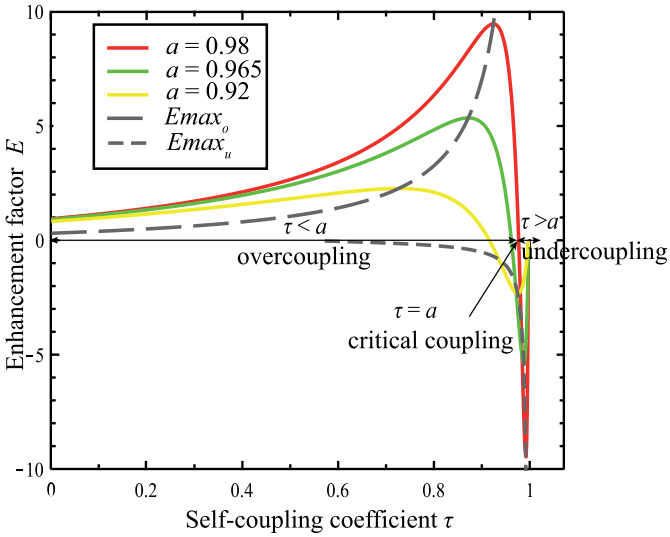

Fig. 3. Enhancement factor E variations versus the self-coupling coefficient τ and in grey dash line, $E_{\max_{o,u}}$ versus the self-coupling coefficient $\tau_{o,u}$ for an all-pass ring resonator with a radius of 15 μm.

B. Enhancement Factor

The sensitivity is the product of a waveguide factor (W) and an enhancement factor (E). The waveguide factor is proportional to the ring path L, the ratio of guided power into the top cladding Γ_{cladd} and inversely proportional to the resonant wavelength λ_{res}. In the following study, L is considered as a physical parameter, Γ_{cladd} is set by the chosen geometry of the waveguide described in Fig. 1 and is equal to 0.25, λ_{res} is set at 532 nm to perform the colorimetric sensing of Chromium Cr (VI) as proposed in [12]. We can note that the optical transducer design could be modified to enhance Γ_{cladd} since the higher Γ_{cladd} the higher the maximum sensitivity [18]. The enhancement factor E is related to the augmentation of the optical path inside the ring resonator and therefore to the ring parameters a and τ.

Two maximum enhancement factors $E_{\max}$ are obtained as shown on Fig. 3. During an over-coupling corresponding to the value τ_o of the self-coupling coefficient, the maximum enhancement factor is called $E_{\max_o}$ and during an under-coupling corresponding to the value τ_u, the maximum enhancement factor is called $E_{\max_u}$. For a resonator with well-known loss coefficient a, we can directly extract the self-coupling coefficients τ_o and τ_u, in case of over-coupling and under-coupling respectively, by

analyzing the derivative of the Eq .8. We obtain $\tau_{o,u}$ as a function of the round-trip loss coefficient a:

$$\begin{cases} \tau_o = -\frac{\sqrt{3}a^2-\sqrt{3}+2a}{a^2-3} & \text{for } a > \frac{1}{\sqrt{3}} \\ \tau_o = 0 & \text{for } a \leq \frac{1}{\sqrt{3}} \\ \tau_u = \frac{\sqrt{3}a^2-\sqrt{3}-2a}{a^2-3} & \text{for } 0 < a < 1 \end{cases} \tag{9}$$

The maximum enhancement factor $E_{\max_{o,u}}$ is defined, as a function of the round-trip loss coefficient a, as follows:

$$\begin{cases} E_{\max_o} = -\dfrac{2a}{3\sqrt{3}(a^2-1)} \\ E_{\max_u} = \dfrac{2a}{3\sqrt{3}(a^2-1)} \end{cases} \tag{10}$$

$E_{\max_{o,u}}$, plotted in grey dash lines in Fig. 3, decrease when a tends towards zero and is the highest when a equal 1.

Positive enhancement factor $E_{\max_o}$ values are obtained when the system is over-coupled ($a > \tau$). In this case, an increase in the propagation losses implies a drop in the transmission and so an increment of the ON-OFF ratio as illustrated in Fig. 2. Once the critical coupling is achieved, the system is under-coupled ($a < \tau$) and negative enhancement factor $E_{\max_u}$ values appear as an increase in the propagation losses induces a reduction of the ON-OFF ratio. The absolute value of the maximum enhancement factor E is the same for under and over-coupling conditions.

If losses are small the single-round optical absorption path can be enhanced up to 10 times for $a = 0.98, \tau_o = 0.95$. Although decreasing overall losses in the ring resonator is crucial to achieve the best sensitivity, the influence of the self-coupling coefficient τ also plays a major role maximizing the performance of the device. By using Eq. 9 and 10, the relation between $E_{\max_{o,u}}$ and $\tau_{o,u}$ is expressed as:

$$\begin{cases} E_{\max_o} = -\frac{(3\tau_o+\sqrt{3})(\tau_o+\sqrt{3})}{9\tau_o^2-9} & \text{for } 0 < \tau_o < 1 \\ E_{\max_u} = -\frac{(3\tau_u-\sqrt{3})(\tau_u-\sqrt{3})}{9\tau_u^2-9} & \text{for } \frac{1}{\sqrt{3}} < \tau_u < 1 \end{cases} \tag{11}$$

The Fig. 3 shows the enhancement factor variations as a function of the self-coupling factor. We have considered different propagation losses leading to different values of a that affect sensor performance. The losses considered in this example are assumed to be due to the intrinsic losses of the material or due to the variable absorption of the top liquid cladding.

It is important to note that for a critical coupling ($\tau = a$) small perturbations in the cladding absorption do not affect significantly the ring transmission by providing a negligible shift in the output power since the major part is lost in the ring. Therefore critical coupling should be avoided for absorption operation contrarily to wavelength-shift sensing techniques. So, in order to increase the sensitivity, over-coupled or under-coupled ring resonators are preferred for absorption spectroscopy. Nonetheless, over-coupling occurs for small gaps between the ring and the waveguide which can be more complex to obtain by photolithography process.

For example, ring resonators presented by Nitkowsky in *et al.* [14] demonstrate a resonance quality factor up to $Q = 120000$.

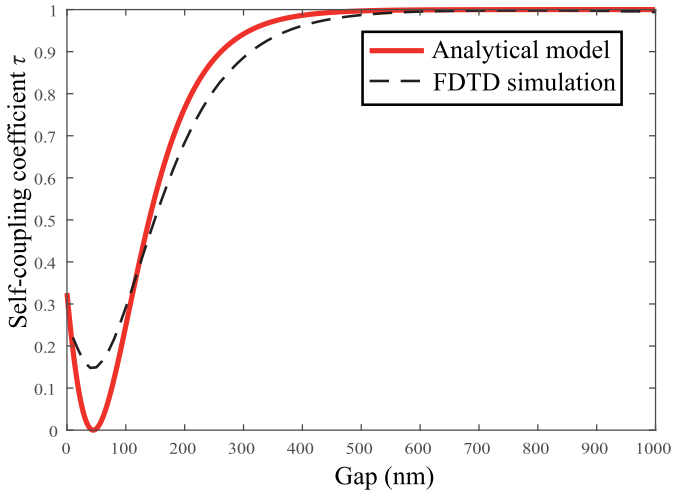

Fig. 4. Variations of self-coupling coefficient τ versus gap for a ring radius of 15 μm. Values found with FDTD simulations and an analytical model based on Marcatili's method [19]–[21] are compared. For the analytical model, it is considered: $A = 0.6\ \mu\text{m}^{-1}$ and $B = 7.3\ \mu\text{m}^{-1}$.

Without any gap optimization the presented devices operate with slightly under-coupled conditions ($a = 0.965, \tau = 0.981$). Such devices exhibited a calculated enhancement factor E of -6 that fully agrees with our predictions as represented by the green curve ($a = 0.965$) in Fig. 3.

For design purpose, the physical parameters of the ring resonator as the gap and the ring radius R are chosen in order to obtain the maximum enhancement factor $E_{\max_{o,u}}$ and therefore the maximum sensitivity $S_{\max_{o,u}}$.

C. Physical Parameters

The maximum sensitivity $S_{\max_{o,u}}$ is given especially by the maximum enhancement factor $E_{\max_{o,u}}$ itself linked to the self-coupling coefficient τ_o and τ_u as previously explained. Fig. 4 represents the self-coupling coefficient versus the gap of the microring resonator calculated by FDTD simulations and the following analytical model based on Marcatili's method [19]–[21]:

$$\tau = \cos^2\left(2\pi A.R \times e^{(-B(R+gap))} \times I_1(B.R)\right) \tag{12}$$

where $I_1(B.R)$ is the Bessel function of the first kind and for B.R$\ll$1, $I_1(B.R)$ is approximated by:

$$I_1(B.R) \simeq \frac{e^{B.R}}{\sqrt{2\pi B.R}}$$

The equation 12 can be expressed as:

$$\tau = \cos^2\left(\frac{A}{\sqrt{B}} \times \sqrt{2\pi R} \times e^{-B.gap}\right) \tag{13}$$

where A and B represent constants, described in the Appendix A, calculating from [19]–[21], depending on the waveguide thickness, width and refractive indexes. Fig. 4 shows that we can extract the $gap_{o,u}$ allowing to have the aimed self-coupling coefficients τ_o and τ_u. For example, in the case of $a = 0.98$ and $\tau_o = 0.95$, shown in Fig. 3, the associated geometric gap_o is found equal to 380 nm. Regardless the values of τ_o and τ_u,

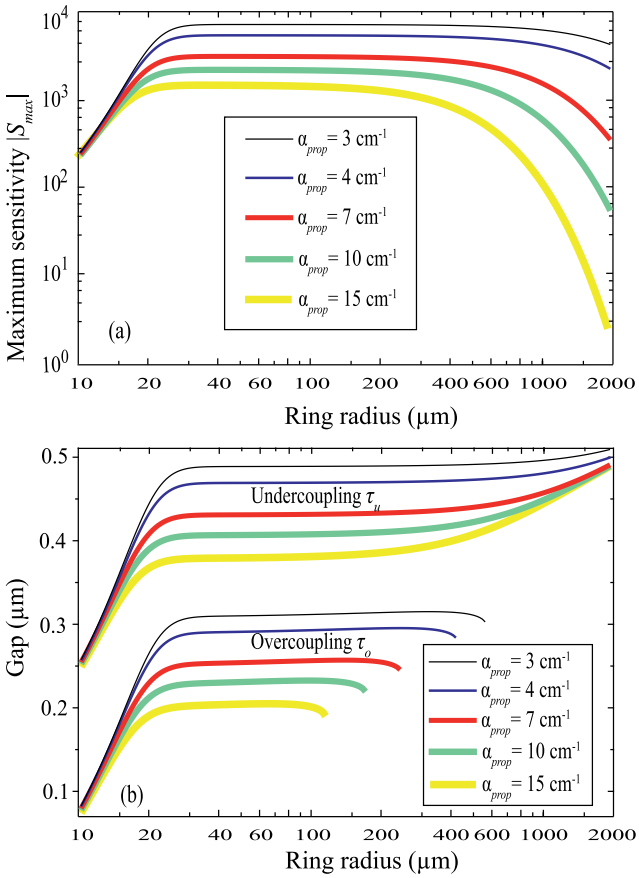

Fig. 5. (a) Maximum sensitivity $\mid S_{\max} \mid$ and (b) $gap_{o,u}$ are represented as a function of the ring radius R for different propagation losses α_{prop} ranging from 3 to 15 cm^{-1}.

thus the micro-resonator can be designed with the adequate gap value.

The maximum sensitivity $S_{\max_{o,u}}$ is given by the following expression:

$$S_{\max_{o,u}} = \pm \frac{4\pi}{\lambda_{res}} L \Gamma_{cladd} \frac{2a}{3\sqrt{3}(a^2-1)} \tag{14}$$

It is well-known that a high sensitivity can be obtained by increasing the ring path L ($=2\pi R$). However, ring resonators with very large radius can lead to dominant propagation losses due to an excessive optical path and an optimum radius must exists depending on the propagation losses. So it is relevant to investigate on the influence of the ring radius for different propagation losses α_{prop} in the ring resonator on the maximum sensitivity $S_{\max}$ in Fig. 5(a). For the simulations of $S_{\max}$ versus the ring radius, it is considered a factor $\Gamma_{cladd} = 0.25$ with $\lambda = 532$ nm. When the ring radius is reduced, bent losses α_{bent} are taken into account and are described in Appendix B. For a certain value of small ring radius, the sensitivity decreases sharply as the bent losses α_{bent} become dominant. As the ring radius increases, there is a ring radius whose value depends on propagation losses α_{prop} and from which the sensitivity dramatically decreases since device propagation losses α_{prop} become high. It exists a range radius allowing the obtention of a maximum and constant sensitivity. For example considering $\alpha_{prop} = 10$ cm^{-1}, the range of radius is 25 μm to 400 μm. This

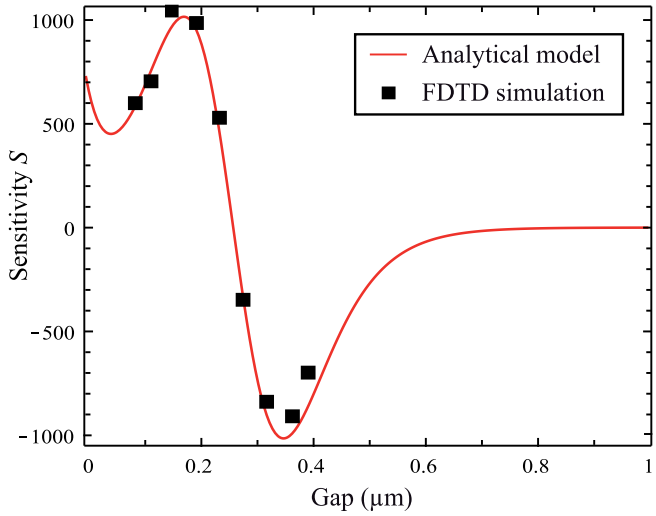

Fig. 6. Variations of sensitivity versus gap : comparison between the proposed analitycal model and the results from the FDTD simulations results.

range radius and the sensitivity increase as losses decrease. If ring resonators are fabricated with low propagation losses, the device footprint can be extended while maintaining maximum performance. However, the free spectral range (FSR) is inversely proportional to the optical path, thus large radius provides closer resonances that can decrease the ON-OFF ratio of the micro-resonator if the quality factor Q is too low.

Each maximum sensitivity $S_{\max_{o,u}}$ is related with an optimal $gap_{o,u}$ that is plotted as a function of the ring radius on Fig. 5(b). As for the sensitivity, a range radius, beginning with a ring radius for which the waveguide bent losses are negligible, permits to achieved the optimal $gap_{o,u}$. When the propagation losses increase, a reduction of the optimal gap is required to compensate the energy loss while maintaining the optimal efficiency. For gap_u, the maximum limit value of the range radius is given by the one of the sensitivity maximum. For gap_o, the range is restricted as $\tau_o = 0$ when round-trip loss coefficient becomes less than $\frac{1}{\sqrt{3}}$. For example, a microring resonator with propagation losses of $\alpha_{prop} = 3$ cm^{-1}, the maximal sensitivity is obtain for a radius of 53 μm and the optimal $gap_{o,u}$ are equal to 310 et 490 nm, respectively. As the losses decreases, the gap increases releasing fabrication process constraints.

IV. Validity of the Model

We calculate the response of a ring resonator with the geometry considered in Section II with a ring radius of 15 μm, $\alpha_{bent} = 14.7$ cm^{-1} and $\alpha_{prop} = 7$ cm^{-1} leading to $a = 0.9$. With a 2.5 FDTD software, we simulate the difference between the transmission of the ring resonator with water cladding and when the cladding is modified by $\Delta n_i = 10^{-5}$. This difference is extracted at resonance. The power drop is calculated considering different gap sizes at resonance wavelength ($\lambda = 532$ nm). The proposed analytical model used Eq. 8 to calculate sensitivity as a function of the self-coupling coefficient τ then Eq. 13 to obtain sensitivity versus gap. Results obtained from FDTD simulations results are compared to the analytical model and plotted in Fig. 6.

The values provided by the FDTD simulations are in good agreement with the ones obtained according Eq. 8 that allows to avoid time-consuming computations. Fig. 3 suggested that it is more difficult to place at maximum undercoupling $E_{\max_u}$ than overcoupling maximum $E_{\max_o}$. As shown in Fig. 6, the full width at half maximum (FWHM) of sensitivity versus gap is the same between over- and under-coupling.

In order to compare these results, full experimental results are needed and require repeatable fabrication process controlling accurately the gap width.

V. Conclusion

We have presented an analytical approach for the microring resonator performance as microspectrometers which provides the theoretical support for the experimental works referred in the literature. From the structure and the propagation losses of the waveguide, this analytical approach permits to obtain both the optima ring radius and gap of the microring resonator in order to obtain a maximal sensitivity for absorption spectroscopy. We demonstrate that such an approach allows significantly to reduce time of FDTD computations and define a range of ring radius to get a maximal sensitivity. A minimal ring radius below which the bent radius losses are dominant and a maximal ring radius beyond which the propagation losses become preponderant. Similar to the optical path based sensors, low-propagation losses are the main requirements to obtain the best performance and so the largest possible ring radius range. Nonetheless, in this work we report additional considerations regarding especially the coupling parameters. Under-coupled resonators, allowing larger gaps, should be preferred instead of the hardly feasible critical coupling. This criterion is of main importance saving worthless optimization efforts during the fabrication steps which would not provide better sensing performance. The results provided by our developed model show both well agreement to experimental results reported in literature and FDTD simulations. Considering the discussed sensing strategy, state-of-the-art propagation loss devices lead to optical path enhancements up to 10 times a single round-trip. For large radius ring resonators ($R > 100$ μm) it implies mm-sized optical paths as found in commercial spectrometers. These results support the use of ring resonators as microspectrometers for applications requiring the handling of resonator footprint-like volumes of liquids while providing a feasible integration within small packages.

Appendix A
Expression of Self-Coupling Coefficient Based on Marcatili's Method [19]–[21]

Using analytical model based on Marcatili's method [19]–[21], we obtain the following self-coupling coefficient, simplified from Eq. (12):

$$\tau = \cos^2\left(\frac{A}{\sqrt{B}} \times \sqrt{2\pi R} \times e^{-B.gap}\right) \tag{15}$$

The constant A is expressed by:

$$A = \frac{k_x^2}{\sqrt{k_1^2 - k_x^2 - k_y^2}} \frac{2B}{a} \frac{1}{a(B^2 + k_x^2)(1 + \frac{2}{aB})} \tag{16}$$

and the constant B is expressed by:

$$B = \frac{\pi}{A_3}\sqrt{1 - \left(\frac{k_x A_3}{\pi}\right)^2} \tag{17}$$

where:

- a is the core waveguide width
- b is the core waveguide height
- n_1 is equal to $n_{co} = 1.56$
- n_2 is equal to $n_{cl} = 1.34$
- n_3 is equal to $n_w = 1.33$
- λ is the wavelength
- k_i are the propagation constants in the free space medium of refractive index n_i :

$$k_i = \frac{2\pi}{\lambda} n_i \tag{18}$$

- A_i are the coefficients given by:

$$A_i = \frac{\pi}{\sqrt{k_1^2 - k_i^2}} \tag{19}$$

- k_x and k_y are the transverse propagation constants respectively:

$$\begin{cases} k_x = \dfrac{\pi}{a}\left(1 + \dfrac{2n_3^2 A_3}{\pi n_1^2 a}\right)^{-1} \\ k_y = \dfrac{\pi}{b}\left(1 + \dfrac{A_2 + A_3}{\pi b}\right)^{-1} \end{cases} \tag{20}$$

Appendix B
Expression of Curvature Losses Calculated by FDTD Simulations

The bent losses α_{bent} used for the simulations in Fig. 5 are calculated by FDTD simulations. They are expressed by:

$$\alpha_{bent} = A \exp\left(-B \times R\right) \tag{21}$$

with $A = 2974$ cm^{-1} and $B = 0.354$ μm^{-1}. R, the ring radius of the microring resonator, is expressed in micrometers.

References

[1] M. A. Pérez, O. González, and J. R. Arias, "Optical fiber sensors for chemical and biological measurements," in *Proc. Curr. Develop. Opt. Fiber Technol.* InTech, 2013.

[2] S. R. Cordero, M. Beshay, A. Low, H. Mukamal, D. Ruiz, and R. A. Lieberman, "A distributed fiber optic chemical sensor for hydrogen cyanide detection," in *Proc. Adv. Environ., Chem. Biol. Sens. Technol. III*, vol. 5993. Int. Soc. Opt. Photon., 2005, Paper 599302.

[3] C.-S. Chu and Y.-L. Lo, "Fiber-optic carbon dioxide sensor based on fluorinated xerogels doped with HPTS," *Sens. Actuators B: Chem.*, vol. 129, no. 1, pp. 120–125, 2008.

[4] M. F. Khanfar, W. Al-Faqheri, and A. Al-Halhouli, "Low cost lab on chip for the colorimetric detection of nitrate in mineral water products," *Sensors*, vol. 17, no. 10, 2017, Art. no. 2345.

[5] J. Godin, C.-H. Chen, S. H. Cho, W. Qiao, F. Tsai, and Y.-H. Lo, "Microfluidics and photonics for bio-system-on-a-chip: A review of advancements in technology towards a microfluidic flow cytometry chip," *J. Biophoton.*, vol. 1, no. 5, pp. 355–376, 2008.
[6] C. Delezoide *et al.*, "Vertically coupled polymer microracetrack resonators for label-free biochemical sensors," *IEEE Photon. Technol. Lett.*, vol. 24, no. 4, pp. 270–272, Feb. 2012.
[7] Y. Sun and X. Fan, "Optical ring resonators for biochemical and chemical sensing," *Anal. Bioanal. Chem.*, vol. 399, no. 1, pp. 205–211, 2011.
[8] M. W. Royal, N. M. Jokerst, and R. B. Fair, "Droplet-based sensing: optical microresonator sensors embedded in digital electrowetting microfluidics systems," *IEEE Sensors J.*, vol. 13, no. 12, pp. 4733–4742, Dec. 2013.
[9] C.-Y. Chao, W. Fung, and L. J. Guo, "Polymer microring resonators for biochemical sensing applications," *IEEE J. Sel. Topics Quantum Electron.*, vol. 12, no. 1, pp. 134–142, Jan./Feb. 2006.
[10] I. Artundo, "Photonic integration: New applications are visible," *Optik Photonik*, vol. 12, no. 3, pp. 22–25, 2017.
[11] M. Diez *et al.*, "Direct patterning of polymer optical periodic nanostructures on cytop for visible light waveguiding," *Opt. Mater.*, vol. 82, pp. 21–29, 2018.
[12] F. Meziane *et al.*, "Study of a polymer optical microring resonator for hexavalent chromium sensing," *Sens. Actuators B: Chem.*, vol. 209, pp. 1049–1056, 2015.
[13] Y. Wang, M. Huang, X. Guan, Z. Cao, F. Chen, and X. Wang, "Determination of trace chromium (VI) using a hollow-core metal-cladding optical waveguide sensor," *Opt. Exp.*, vol. 21, no. 25, pp. 31 130–31 137, 2013.
[14] A. Nitkowski, A. Baeumner, and M. Lipson, "On-chip spectrophotometry for bioanalysis using microring resonators," *Biomed. Opt. Express*, vol. 2, no. 2, pp. 271–277, 2011.
[15] C.-Y. Chao and L. J. Guo, "Design and optimization of microring resonators in biochemical sensing applications," *J. Lightw. Technol.*, vol. 24, no. 3, pp. 1395–1402, Feb. 2006.
[16] A. Nitkowski, L. Chen, and M. Lipson, "Cavity-enhanced on-chip absorption spectroscopy using microring resonators," *Opt. Express*, vol. 16, no. 16, pp. 11 930–11 936, 2008.
[17] W. Bogaerts *et al.*, "Silicon microring resonators," *Laser Photon. Rev.*, vol. 6, no. 1, pp. 47–73, 2012.
[18] S. M. Lo, S. Hu, G. Gaur, Y. Kostoulas, S. M. Weiss, and P. M. Fauchet, "Photonic crystal microring resonator for label-free biosensing," *Opt. Express*, vol. 25, no. 6, pp. 7046–7054, 2017.
[19] E. Marcatili, "Dielectric rectangular waveguide and directional coupler for integrated optics," *Bell Syst. Tech. J.*, vol. 48, pp. 2071–2102, 1969.
[20] M. Kuznetsov, "Expressions for the coupling coefficient of a rectangular-waveguide directional coupler," *Opt. Lett.*, vol. 8, no. 9, pp. 499–501, 1983.
[21] P. Girault *et al.*, "Integrated polymer micro-ring resonators for optical sensing applications," *J. Appl. Phys.*, vol. 117, no. 104504, pp. 1–8, 2015.

Miguel Diez Garcia received the M.Sc. degree in optoelectronics from the University of Montpellier, Montpellier, France, in 2015, and the Ph.D degree in photonics from the University of Bordeaux, Bordeaux, France, in 2018. He participated in several projects in fabrication test and development of optical based devices. He is specialized in evanescent integrated optical sensors and interferometric sensors.

Pauline Girault is 28 years old. She received the M.Sc. degree in nanotechnologies from the University of Nantes, Nantes, France, in 2013, and the Ph.D. degree in physics from the University of Rennes, Rennes, France, in 2016. Since 2017, she has continued, in a Postdoctoral Position, her Ph.D study on integrated micro-resonator based on polymer and porous silicon for sensor applications at FOTON institute, Lannion, France. Her current postdoctoral research interests, at IMS Laboratory, Talence, France, involve the implementation and characterization of a portable, robust and sensitive polymer-based photonic sensor for environmental pollutant detection.

Simon Joly is 37 years old. He received the Ph.D. degree in physics from the University of Grenoble, Grenoble, France, in 2009. Since 2013, he has been an Associate Professor with the University of Bordeaux in IMS laboratory, Talence, France. From 2010 to 2013, he undertook three postdoctoral positions, at the Institute of Molecular Science in Japan, at the IMEP-LAHC laboratory, then at the CEA in France. He has been involved in nonlinear optics, laser, terahertz spectroscopy, and infrared imaging research activities. His current research concerns evaluation of photonics components within the EDMINA Research Group at the Integration of Material to System Laboratory (IMS).

Laurent Oyhenart received the Ph.D. degree in electrical engineering from the University of Bordeaux, Bordeaux, France, in 2005. He is currently an Associate Professor with the University of Bordeaux and develops his research activities in the IMS laboratory. His research interests include computational electromagnetics, photonic crystals, and energy harvesting.

Vincent Raimbault has been a CNRS researcher since 2010. He is currently working with the LAAS CNRS laboratory on the development of sensing systems for environmental analysis, by using the combination of microfluidics and microsensors. He has worked on a variety of sensing technologies including acoustic Love waves, electrochemical, optical micro-ring resonators and miniaturized absorption spectroscopy, as well as alternative fabrication techniques for microfluidics (laminated dry films, micrometric-resolution 3-D printing).

Corinne Dejous received the electronics engineer degree from the French "Grande Ecole" ENSEIRB in 1991 and the Ph.D. degree from the University of Bordeaux, Bordeaux, France, in 1994. She is currently a full-time Professor with Bordeaux INP and conducts her research at the Integration from Materials to Systems Laboratory (IMS, CNRS UMR 5218). She was the head of the "Microsystems" research group of IMS from 2011 to 2018 and is currently in charge of the transverse axis of IMS on Environments. Her research interest mainly aims the development of (bio)chemical microsensing platforms based on acoustic waves and more generally on wave-based resonant devices, mostly for health and environment real-time monitoring.

Laurent Bechou received the Ph.D. degree in electronics from the University of Bordeaux, Bordeaux, France, in 1998. Then, he joined the Integration of Material to System Laboratory (IMS) at the University of Bordeaux 1 as an Associate Professor. Since 2010, he has been a Full Professor in electronics and physics with the University of Bordeaux. Since 2010, he has been the head of the Reliability Assessment of Micro and Nano-assemblied Devices research group (EDMINA) at IMS. He is the author or coauthor of more than 180 regular papers and international conferences. Since March 2016, he has been appointed as an Associated Professor with the French-Canadian Joint Lab CNRS LN2-University of Sherbrooke (QC, Canada) working on packaging and design for reliability of devices and systems for photonic applications, co-leader of the Packaging research group. His research interests focus on design for reliability including design, fabrication, characterization and aging effects of packaged optoelectronic and photonic devices based on physics of the light-matter interactions as well as the understanding of early degradation processes.